Remote Sensing of Environment 139 (2013) 116–129

Contents lists available at ScienceDirect

Remote Sensing of Environment

journal homepage: www.elsevier.com/locate/rse

# High spatial resolution mapping of elevated atmospheric carbon dioxide using airborne imaging spectroscopy: Radiative transfer modeling and power plant plume detection

Philip E. Dennison [a,*], Andrew K. Thorpe [b], Eric R. Pardyjak [c], Dar A. Roberts [b], Yi Qi [a], Robert O. Green [d], Eliza S. Bradley [b], Christopher C. Funk [b]

[a] Department of Geography, University of Utah, 260 S Central Campus Dr., Room 270, Salt Lake City, UT 84112, USA
[b] Department of Geography, University of California Santa Barbara, Santa Barbara, CA 93106, USA
[c] Department of Mechanical Engineering, University of Utah, Salt Lake City, UT 84112, USA
[d] Jet Propulsion Laboratory, California Institute of Technology, Pasadena, CA 91109, USA

ARTICLE INFO

*Article history:*
Received 28 October 2012
Received in revised form 25 June 2013
Accepted 1 August 2013
Available online 30 August 2013

*Keywords:*
AVIRIS C
AVIRIS NG
MODTRAN
Noise equivalent delta radiance
Hyperspectral data
Imaging spectroscopy
$CO_2$ emissions
Fossil fuel power plant

ABSTRACT

Carbon dioxide is emitted from the combustion of fossil fuels and is an important contributor to anthropogenic climate change. Multiple current and planned satellite missions are designed to quantify atmospheric carbon dioxide concentrations on a global scale, but most of these sensors do not have the spatial resolution necessary to resolve point sources such as fossil fuel power plants. Airborne imaging spectrometer data, such as those from the Airborne Visible InfraRed Imaging Spectrometer (AVIRIS), can have multiple, contiguous bands covering shortwave infrared (SWIR) absorption features produced by carbon dioxide. Therefore, high spatial resolution data from AVIRIS-like sensors may offer a means for detecting plumes and retrieving carbon dioxide concentrations for point source emissions. The objectives of this study include modeling minimum carbon dioxide anomalies detectable in AVIRIS data under different conditions and applying a Cluster-Tuned Matched Filter for detection of carbon dioxide plumes in simulated data and in AVIRIS images acquired over power plants. Radiative transfer simulations were used to model the residual radiance produced by increased absorption by carbon dioxide as concentration was elevated above background levels within a 0–500 m layer. Carbon dioxide anomalies, surface reflectance, water vapor concentration, solar zenith angle, sensor height, and aerosol scattering were varied in simulation sets and the resulting residual radiance spectra were compared against noise equivalent delta radiance (NEdL) for the "classic" and "next generation" AVIRIS instruments. Sensitivity to carbon dioxide anomalies improved with increased surface reflectance and declined with increased water vapor concentration, solar zenith angle, sensor height, and aerosol scattering. Zero to 500 m concentration anomalies as low as 100 parts per milion by volume (ppm) for AVIRIS C and 25 ppm for AVIRIS NG produced residual radiance values that exceeded SWIR NEdL. Carbon dioxide concentrations modeled for a generic power plant emissions scenario using a plume dispersion model were combined with randomly-generated reflectance spectra to create simulated images with varying surface reflectance and NEdL. For these simulated images, true positive and false positive detection rates improved as background reflectance increased and as NEdL decreased. Apparent plumes were detected in all four AVIRIS C images acquired over power plants, although the characteristics of the plumes varied according to solar-plume-sensor geometry. Improvements in modeling may allow retrieval of plume concentration, providing a valuable means for quantifying point source emissions and a basis for comparison with column concentrations retrieved from in situ measurements and coarse resolution satellite data.



## 1. Introduction

Greenhouse gases affect Earth's energy balance by absorbing outgoing longwave radiation. Anthropogenic increases in the atmospheric concentration of multiple greenhouse gases, including carbon dioxide ($CO_2$), methane ($CH_4$), nitrous oxide ($N_2O$), and halocarbons, have caused positive radiative forcing resulting in increased global temperature (Forster et al., 2007). Of the long-lived greenhouse gases, carbon dioxide has contributed the most radiative forcing since the start of the industrial era. Pre-industrial atmospheric concentrations are estimated between 275 and 285 parts per milion by volume (ppm) (Forster et al., 2007). Cumulative emissions from fossil fuel combustion and cement production have exceeded 350 billion tons of carbon (Boden, Marland, & Andres, 2011), resulting in a global average carbon dioxide concentration surpassing 390 ppm in 2012 (NOAA, 2012).

* Corresponding author. Tel.: +1 801 585 1805.
*E-mail address:* dennison@geog.utah.edu (P.E. Dennison).

0034-4257/$ – see front matter © 2013 Elsevier Inc. All rights reserved.
http://dx.doi.org/10.1016/j.rse.2013.08.001

Increasing population and demand for electricity has resulted in increased global energy consumption, with the global annual primary energy supply nearly doubling between 1973 ($2.56 \times 10^{20}$ J) and 2009 ($5.09 \times 10^{20}$ J) (IEA, 2011). The dominant source of electricity generation is power plant combustion of fossil fuels, resulting in point source emission that comprises a significant share of global anthropogenic carbon dioxide emissions. Within the United States, 40.6% of $CO_2$ emissions are attributed to stationary sources that generate electricity by combusting fossil fuels (EPA, 2012). Emission estimates from power plants can have large uncertainties; for example, Ackerman and Sundquist (2008) found a 16.9% average absolute difference for emission estimates from the U.S. Department of Energy's Energy Information Administration (EIA) and the U.S. Environmental Protection Agency's eGRID database. In the U.S., uncertainty in fossil fuel carbon dioxide emissions was estimated to be between −1 and 6% (EPA, 2011). For the EU-25 nations emission uncertainty was 7% when comparing four inventory methods (Ciais et al., 2010), and between 15 and 20% for China when including both fossil fuel consumption and cement production (Gregg, Andres, & Marland, 2008).

Given these uncertainties, there is increased interest in developing methods of quantifying anthropogenic carbon dioxide emissions using remote sensing. Past and ongoing satellite missions have provided the ability to monitor global carbon dioxide concentrations at coarse spatial resolutions, including the Atmospheric Sounding Interferometer (IASI; Crevoisier et al., 2009), the Atmospheric Infrared Sounder (AIRS; Jiang, Chahine, Olsen, Chen, & Yung, 2010), the Tropospheric Emission Spectrometer (TES; Kulawik et al., 2010), the Scanning Imaging Absorption Spectrometer for Atmospheric Chartography (SCIAMACHY; Schneising et al., 2008), and the Greenhouse Gas Observing Satellite (GOSAT; Saitoh, Imasu, Ota, & Niwa, 2009). In addition to detecting temporal and spatial variability in carbon dioxide concentrations, data like those provided by SCIAMACHY and GOSAT have great potential for estimating surface fluxes by inverse modeling of satellite observations (Chevallier et al., 2009; Schneising et al., 2012). Scheduled for launch in 2014, the Orbiting Carbon Observatory (OCO)-2 is equipped with a near infrared (NIR)/SWIR spectrometer that should provide a 1 ppm column concentration accuracy and km-scale spatial resolution needed for constraining regional sources and sinks (Crisp et al., 2004). Further, space-based detection of carbon dioxide emissions from power plants appears feasible using the proposed Carbon Monitoring Satellite (CarbonSat; Velazco et al., 2011).

Airborne sensors offer the potential to better constrain local emissions and improve greenhouse gas budgets (NRC, 2010). Recently developed airborne sensors have great potential for measuring carbon dioxide emissions at local and regional scales while complementing global monitoring efforts at coarser resolutions. For example, the non-imaging SWIR spectrometer MAMAP (Methane Airborne MAPper) has been used to measure a carbon dioxide plume emitted from a coal-fired power plant (Bovensmann et al., 2010). As part of the Carbon in Arctic Reservoirs Vulnerability Experiment (CARVE), a nadir-viewing Fourier transform spectrometer (FTS) is being used to measure total atmospheric columns of carbon dioxide in Alaskan terrestrial ecosystems (Miller & Dinardo, 2012). However, these sensors provide atmospheric column concentrations for a small footprint; MAMAP is non-imaging and has a ground sample distance of approximately 33 m for a 1 km flight height (Gerilowski et al., 2011), while the FTS telescope for the CARVE mission has a 10° field of view with a spatial resolution approximately 100 × 1000 m (Miller & Dinardo, 2012).

The finer spatial resolution Airborne Visible InfraRed Imaging Spectrometer (AVIRIS) measures reflected solar radiance across 224 contiguous spectral bands between 350 and 2500 nm with a 10 nm spectral sampling (Green, Eastwood, & Williams, 1998). For the "classic" AVIRIS instrument (AVIRIS C) spatial resolution typically ranges between 3 and 20 m depending on platform altitude, while the "next generation" AVIRIS instrument (AVIRIS NG) is capable of spatial resolutions as fine as 1 m with an improved spectral sampling of 5 nm. The objectives of this study are to establish minimum carbon dioxide anomalies as thresholds for plume detection, and to demonstrate carbon dioxide plume detection in simulated images and in AVIRIS C data acquired over power plants. Using radiative transfer modeling, we compare residual radiance caused by increased carbon dioxide absorption to noise equivalent delta radiance for AVIRIS C and AVIRIS NG. Simulated images and AVIRIS C images acquired over four U.S. power plants are used to demonstrate carbon dioxide plume detection based on a Cluster-Tuned Matched Filter (CTMF) approach.

## 2. Background

In addition to strong vibrational absorptions in the mid infrared and longwave (thermal) infrared, carbon dioxide has distinct vibrational–rotational absorptions in the SWIR. Fig. 1 shows modeled atmospheric transmittance for the three primary greenhouse gases: carbon dioxide, methane, and water vapor. These transmittance spectra were generated using the MODTRAN radiative transfer model (Berk, Bernstein, & Robertson, 1989) and convolved to the 10 nm spectral sampling of AVIRIS C. The strongest carbon dioxide absorptions peak at approximate wavelengths of 1960, 2010, and 2060 nm. At shorter wavelengths in this range, carbon dioxide absorption features overlap with strong water vapor absorption (Fig. 1). Weaker carbon dioxide absorption features present at 1570 and 1600 nm are free of strong water vapor absorption, but the absorption feature at 1430 nm is completely within a strong water vapor absorption band.

Imaging spectrometer data that include carbon dioxide SWIR absorption bands have potential for mapping spatial variation in atmospheric carbon dioxide concentration. Absorption of reflected solar radiance occurs for both direct and scattered radiance, complicating measurement of the carbon dioxide absorption signal. Solar zenith angle, view zenith angle, sensor height, and surface elevation determine the length of the direct path. These factors, along with scattering and absorption by water vapor and aerosols, influence carbon dioxide absorption of scattered radiance. While the length of the direct path is usually known, aerosol and water vapor effects are often unknown and must be measured. Atmospheric pressure and temperature also impact carbon dioxide absorption through broadening of absorption lines at higher pressures and temperatures. All radiance measured by a sensor is normally assumed to be solar radiance, but emitted radiance can significantly reduce apparent carbon dioxide absorption by greatly reducing path length (Dennison, 2006). Reduction in carbon dioxide absorption due to emitted radiance provides a means for fire detection using imaging spectrometer data (Dennison, 2006; Dennison & Roberts, 2009; Matheson & Dennison, 2012).

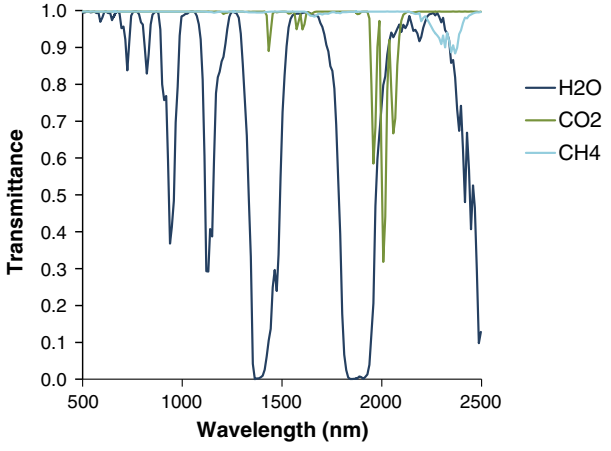


**Fig. 1.** Atmospheric transmittance for the three primary greenhouse gases, based on a MODTRAN simulation convolved to the 2011 AVIRIS C sensor response function.